



Comparative Study on the Regeneration of Fe₃O₄@Graphene Oxide Composites

Zhongliang Hu*, Xiaojing Zhang, Jingying Li and Yirong Zhu*

Department of Inorganic Nonmetallic Material, College of Metallurgy and Material Engineering, Hunan University of Technology, Zhuzhou, China

In this study, two kinds of composites with the structure of graphene oxide (GO) sheets wrapped magnetic nanoparticles were investigated on their regeneration. The composites have a similar core-shell structure, but the interactions between the core and shell are quite different, which are electrostatic and covalent. They were characterized by scanning/transmission electron microscopy, power X-ray diffraction, and vibrating sample magnetometer analysis. Their morphologies and structures of the samples had been revealed using methylene blue and Pb(II) as adsorbates during regeneration. The results showed that the composites with covalent bonding interaction could maintain a stable core-shell structure and present a good regeneration performance for adsorption-desorption of methylene blue and Pb(II). The composites with electrostatic interaction could approximately preserve its core-shell structure and could be recyclable for adsorption-desorption of methylene blue, however, they would disintegrate its core-shell structure during adsorption/desorption of Pb(II), thus greatly decreasing their regeneration performance. The regeneration mechanisms of the composites were analyzed, which could provide a useful theoretical guide to design the GO sheets wrapped magnetic nanoparticles composites.

OPEN ACCESS

Edited by:

Angang Dong,
Fudan University, China

Reviewed by:

Huaibin Shen,
Henan University, China
Yanbin Cui,
Institute of Process Engineering
(CAS), China

*Correspondence:

Zhongliang Hu
david10103@sina.com
Yirong Zhu
zhuyirong2004@163.com

Specialty section:

This article was submitted to
Nanoscience,
a section of the journal
Frontiers in Chemistry

Received: 12 December 2019

Accepted: 17 February 2020

Published: 28 February 2020

Citation:

Hu Z, Zhang X, Li J and Zhu Y (2020)
Comparative Study on the
Regeneration of Fe₃O₄@Graphene
Oxide Composites.
Front. Chem. 8:150.
doi: 10.3389/fchem.2020.00150

Keywords: graphene oxide, regeneration, Fe₃O₄, core-shell structure, magnetic graphene based composites

INTRODUCTION

Due to the unique structure and excellent characteristics, graphene and its derivatives have attracted more and more interests in the scientific community (Geim and Novoselov, 2007; Smith and Rodrigues, 2015; Nandhanapalli et al., 2019). Recently, graphene-based composites have been largely investigated as adsorption materials, which displayed excellent performances for adsorption of heavy metal ions, organic and dyes (Mi et al., 2012; Sitko et al., 2013; Yoon et al., 2016; Liu et al., 2018; Li et al., 2019). Notably, magnetic graphene oxide (GO) composites have been regarded as promising adsorbents for water purification because they could be easily separated from solution under an external magnetic field, thus overcoming the limitation of GO's difficult separation in solution (Chandra et al., 2010; He et al., 2010; Ma et al., 2018). However, GO sheets tend to restack, thus inevitably reducing their surface area and adsorption capacity (Bourlinos et al., 2003).

To further improve the performance, some researchers have attempted to wrap Fe₃O₄ nanoparticles (NPs) with GO sheets and the obtained GO@Fe₃O₄ displayed excellent adsorption performance toward pollutants (Wei et al., 2012; Pan et al., 2016). Compared with the magnetic GO composites where Fe₃O₄ is deposited on GO sheets, the GO@Fe₃O₄ composites have two obvious advantages. Firstly, they have much more stable structure because the connection area between

GO and Fe₃O₄ is much more extensive; secondly, the restacking of GO sheets could be completely avoided, thereby enhancing their performances.

We have synthesized magnetic GO composites as environmental materials recently (Hu et al., 2009, 2010, 2012). Fe₃O₄ NPs have been successfully encapsulated with GO sheets through electrostatic interaction and covalent bonding, and both of the GO-based composites exhibited excellent adsorption toward contaminants in solution (Hu et al., 2017, 2020). Further researches revealed that the two kinds of composites displayed quite different regeneration toward heavy metal ions and organics. It is known that good regeneration is the prerequisite for the commercial application of the GO-based adsorbents due to their relatively high cost. Therefore, the investigations on the regeneration of GO-based adsorbents are very meaningful for related researches. Unfortunately, there exist rarely systematic studies on the regeneration of GO-based composites. Previous surveys only involved their adsorption capacity after several cycles, but the associated regeneration mechanisms including the morphology and structure evolution during regeneration had been scarcely investigated.

In this paper, our investigations are focused on the regeneration processes and the mechanisms of two kinds of Fe₃O₄@GO composites, which had been successfully synthesized in our previous study. Although both of the Fe₃O₄@GO samples have similar a core-shell structure, in which GO sheets are tightly connected with magnetic NPs, the interactions linking the core and shell are quite different, which are electrostatic and covalent, respectively. Methylene blue and Pb(II) were used as typical adsorbates to elucidate the evolution of the morphologies and structures of both samples during regeneration in detail. To the best of our knowledge, it is firstly reported to systematically investigate the regeneration mechanisms of the Fe₃O₄@GO composites, and the study could provide a theoretical guide for improving the regeneration of GO-based composites, thus accelerating their practical application.

EXPERIMENTAL

Materials

Graphite (100 mesh, XFnano), ferric chloride hexahydrate (FeCl₃·6H₂O, Sinopharm), ethylene glycol (Sinopharm), polyethylene glycol (PEG 4000, Sinopharm), sodium acetate trihydrate (NaAc·3H₂O, Sinopharm), tetraethyl orthosilicate (Sinopharm), poly(diallyldimethylammonium chloride) (PDDA, Sinopharm), 3-aminopropyl triethoxysilane (APTES, Sinopharm), 1-ethyl-3-(3-dimethylaminopropyl) carbodiimide hydrochloride (EDC, Sinopharm), n-hydroxysuccinimide (NHS, Sinopharm), ammonia water (28 wt.%, Sinopharm), hydrochloric acid (Sinopharm), lead nitrate [Pb(NO₃)₂, Sinopharm], methylene blue (MB, Sinopharm).

Materials Synthesis

Synthesis of GO Wrapped Fe₃O₄ Composites by Electrostatic Interaction

The synthesis procedures of GO wrapped Fe₃O₄ composites by electrostatic interaction (Fe₃O₄@GO-e) were described

elsewhere in detail (Hu et al., 2020). The preparation steps included synthesis of Fe₃O₄, SiO₂ coating on Fe₃O₄, introduction of PDDA on Fe₃O₄ and encapsulation of GO's sheets on magnetic particles. SiO₂ coating endowed Fe₃O₄ with rich hydrophilic groups such as -OH, which can attract PDDA molecules with positive charges, and the positive charges on Fe₃O₄ could induce the coating of GO's sheets with negative charges, forming a core-shell structure. In brief, solvothermal synthesized Fe₃O₄ NPs were coated with a layer of SiO₂ by a modified Stoker method (Gao et al., 2013), then the surface modified Fe₃O₄ NPs were mixed with PDDA solution. At the same time, the graphite oxide prepared by Hummers' method (Hummers and Offeman, 1958) was dispersed in distilled water. The dispersed GO solution was mixed with the above solution, and reacted for 8h. After washing, separation and drying, Fe₃O₄@GO-e was obtained.

Synthesis of GO Sheets Wrapped Fe₃O₄ Composites by Covalent Bonding

The detailed synthesis processes of GO sheets wrapped Fe₃O₄ composites by covalent bonding (Fe₃O₄@GO-c) could be found elsewhere (Hu et al., 2017), and they were composed of the following steps: synthesis of Fe₃O₄, SiO₂ coating on Fe₃O₄, amination surface on Fe₃O₄ and final coupling reaction between GO and Fe₃O₄. The former procedures of solvothermal synthesis of Fe₃O₄ NPs and subsequent SiO₂ coating were same as those of GO@Fe₃O₄-e except for some parameter modifications. After SiO₂ coating, the amination on the surface of the magnetic NPs was carried out using APTES precursor, thus endowing the magnetic particles with rich amino groups on their surface. Meanwhile, the graphite oxide prepared by Hummers' method was dispersed in distilled water and its pH value was adjusted with a buffer solution. Subsequently, EDC and NHS were added into the GO solution, and finally the mixed solution reacted with aminated Fe₃O₄ NPs, resulting in the formation of Fe₃O₄@GO-c.

Materials Characterization

Scanning electron microscopy (SEM) images were obtained using a JEOL JSM-6360LV or Hitachi S4800. Transmission electron microscope (TEM, Tecnai G2 F20, FEI, USA) was utilized to investigate the morphology and microstructure of the sample. The powder X-ray diffraction (XRD) patterns of the samples were collected from a Bruker D8 advanced diffractometer using Cu-K α radiation ($\lambda = 0.1514$ nm) in the 2θ range of 10–80°. The magnetic experiments were performed on a Lakeshore 7407 vibrating sample magnetometer at room temperature.

Adsorption Experiments

MB, a common dye pollutant, and Pb(II), a typical heavy metal ion, were used as adsorbates for the study. The adsorption experiments were carried out on a shaker with a shaking speed of 200 rpm at 30°C.

For MB adsorption tests, 50 mg of the sample and 50 mL of MB solution (150 mg/L, pH = 8) were mixed in a 100 mL air-tight glass conical flask. The adsorption equilibrium was reached after 2 h of agitation. Subsequently, the adsorbent was separated using a hand-held permanent magnet. The supernatant was collected for concentration measurements

by UV-vis spectrophotometry. The adsorption capacity was calculated based on the following formula:

$$q_e = \frac{(C_0 - C_e)V}{M} \quad (1)$$

where q_e refers to the adsorption equilibrium capacity, C_0 and C_e denote the initial and equilibrium concentrations, respectively, V is the solution volume, and M represents the adsorbent's mass.

For Pb(II) adsorption, the experimental procedures were same as the above ones except for modifications of the following parameters. The initial concentration of Pb(II) solution was 300 mg/L, and its pH value was adjusted to 6 before adsorption tests. The adsorption equilibrium time was set as 12 h. The Pb(II) concentration in the supernatant was measured by atomic absorption spectrophotometry and the adsorption capacity toward Pb(II) was obtained according to Equation (1).

Desorption and Regeneration Experiments

The MB-loaded and Pb(II)-loaded samples were utilized to evaluate the regeneration performance. For MB desorption, the regeneration of the sample was carried out by immersing it in ethanol solution under mechanical stirring for 30 min. For Pb(II) desorption, the regeneration of the sample was performed by soaking it in the presence of 0.01 M of HCl under ultrasonication for 30 min.

RESULTS AND DISCUSSIONS

SEM/TEM Analyses of the Fe₃O₄@GO Samples

SEM/TEM could intuitively reveal the morphologies and textures of the samples. The SEM/TEM images of the Fe₃O₄@GO-e sample are shown in **Figure 1**. From the SEM image (**Figure 1a**), it could be clearly observed that the Fe₃O₄ NPs or Fe₃O₄ NP aggregations are tightly wrapped by the silk-like GO sheets. The TEM images of the sample (**Figures 1b,c**) further demonstrate that the corrugated GO sheets are compactly connected with the magnetic NPs. The high-resolution TEM of the sample is displayed in **Figure 1d**, in which the atomic lattice fringes could be distinctly observed. The interplanar spacing (~ 0.48 nm) could be attributed to the (111) lattice plane of the Fe₃O₄ crystal. In this study, the good structure of the Fe₃O₄@GO-e sample could be ascribed to the utilization of Fe₃O₄ NPs with large surface area, rich -OH groups on the surface introduced by SiO₂ coating, and PDDA with positive charges which could strongly attract the negative GO sheets.

Figure 2 shows the SEM/TEM images of the Fe₃O₄@GO-c sample. Compared with the Fe₃O₄@GO-e sample, Fe₃O₄@GO-c also presents a core-shell structure, where the magnetic NPs are roundly encapsulated by the wrinkled silk-like GO sheets. Its SEM image is similar to Fe₃O₄@GO-e's, indicating that the encapsulation effect of the sample is good as Fe₃O₄@GO-e's. However, the TEM images exhibit that the crinkly GO sheets are more densely and firmly grafted to the magnetic NPs surface, inferring that the sample has a more stable structure than Fe₃O₄@GO-e. The structure difference between two samples

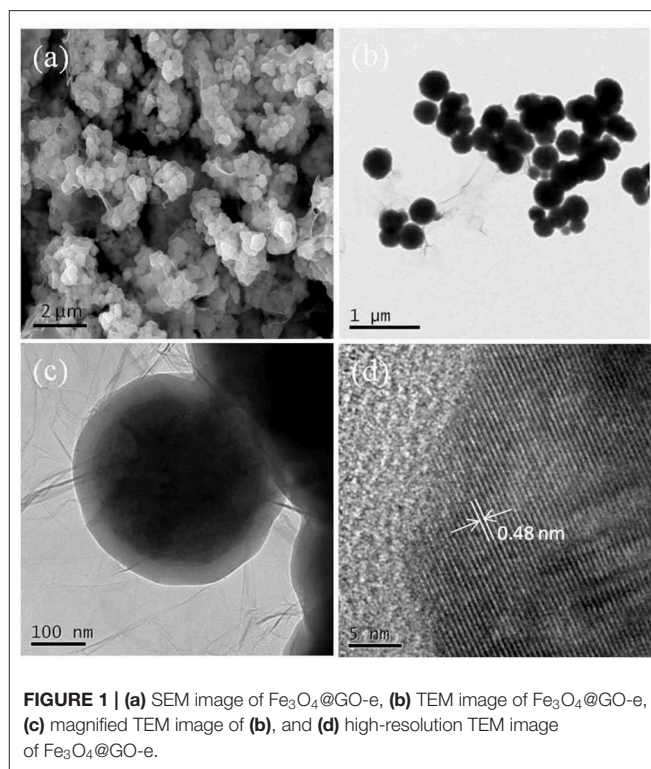


FIGURE 1 | (a) SEM image of Fe₃O₄@GO-e, (b) TEM image of Fe₃O₄@GO-e, (c) magnified TEM image of (b), and (d) high-resolution TEM image of Fe₃O₄@GO-e.

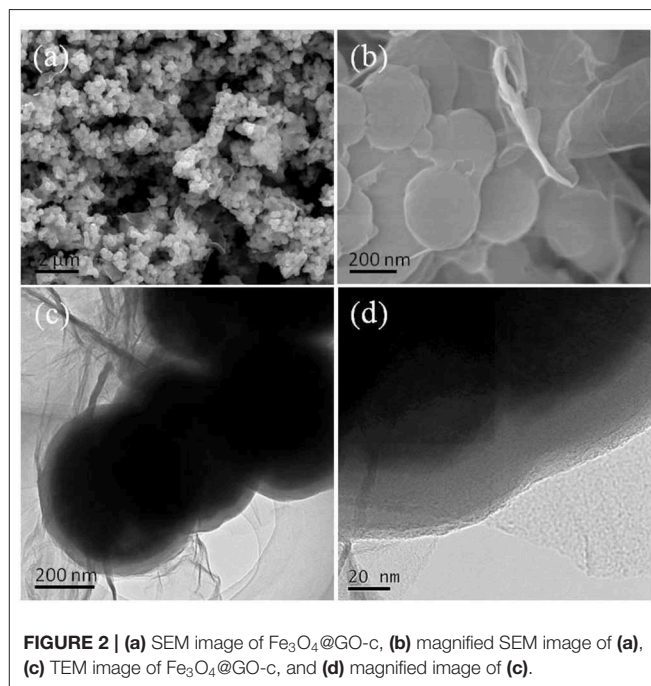


FIGURE 2 | (a) SEM image of Fe₃O₄@GO-c, (b) magnified SEM image of (a), (c) TEM image of Fe₃O₄@GO-c, and (d) magnified image of (c).

could be reasonably deduced that the covalent bonding in Fe₃O₄@GO-c is much stronger than the electrostatic interaction in Fe₃O₄@GO-e. This difference could have a significant influence on their regeneration.

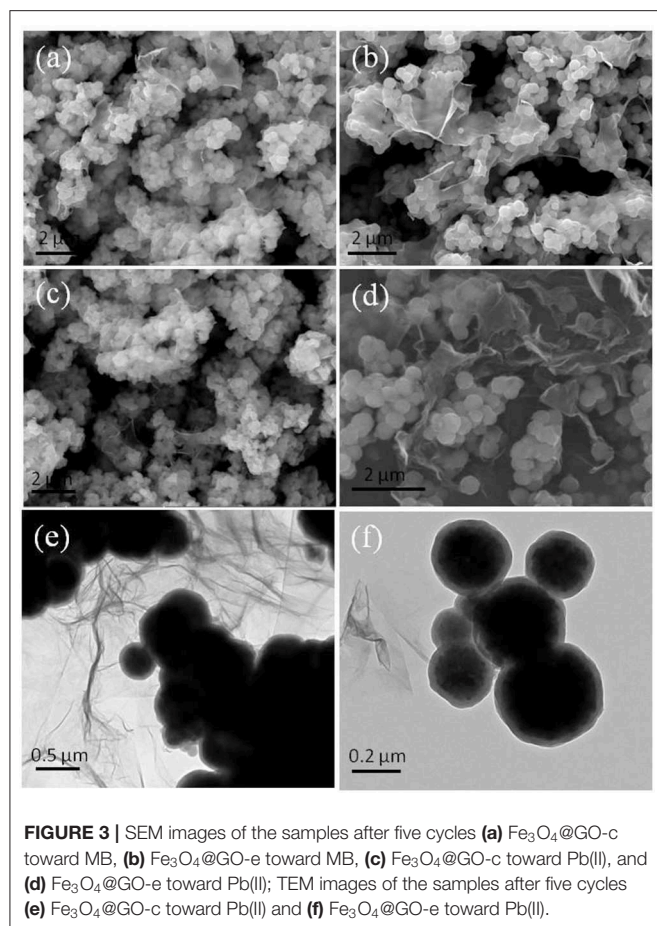


FIGURE 3 | SEM images of the samples after five cycles (a) Fe₃O₄@GO-c toward MB, (b) Fe₃O₄@GO-e toward MB, (c) Fe₃O₄@GO-c toward Pb(II), and (d) Fe₃O₄@GO-e toward Pb(II); TEM images of the samples after five cycles (e) Fe₃O₄@GO-c toward Pb(II) and (f) Fe₃O₄@GO-e toward Pb(II).

Morphology and Structure Analyses of the Fe₃O₄@GO Samples After Regeneration

The regenerability of the sample has much to do with its evolution of morphology and structure during adsorption-desorption recycling. **Figure 3** displays the SEM/TEM images of the samples after five cycles of adsorption-desorption toward MB and Pb(II). Compared with the morphology before adsorption test, the morphology of Fe₃O₄@GO-c changed little (**Figures 3a,c,e**), indicating that it could maintain its structure during regeneration toward MB and Pb(II). As a result, it could be recyclable. The next tests of adsorption-desorption further demonstrate that the stable structure is beneficial to enhancing its regenerability.

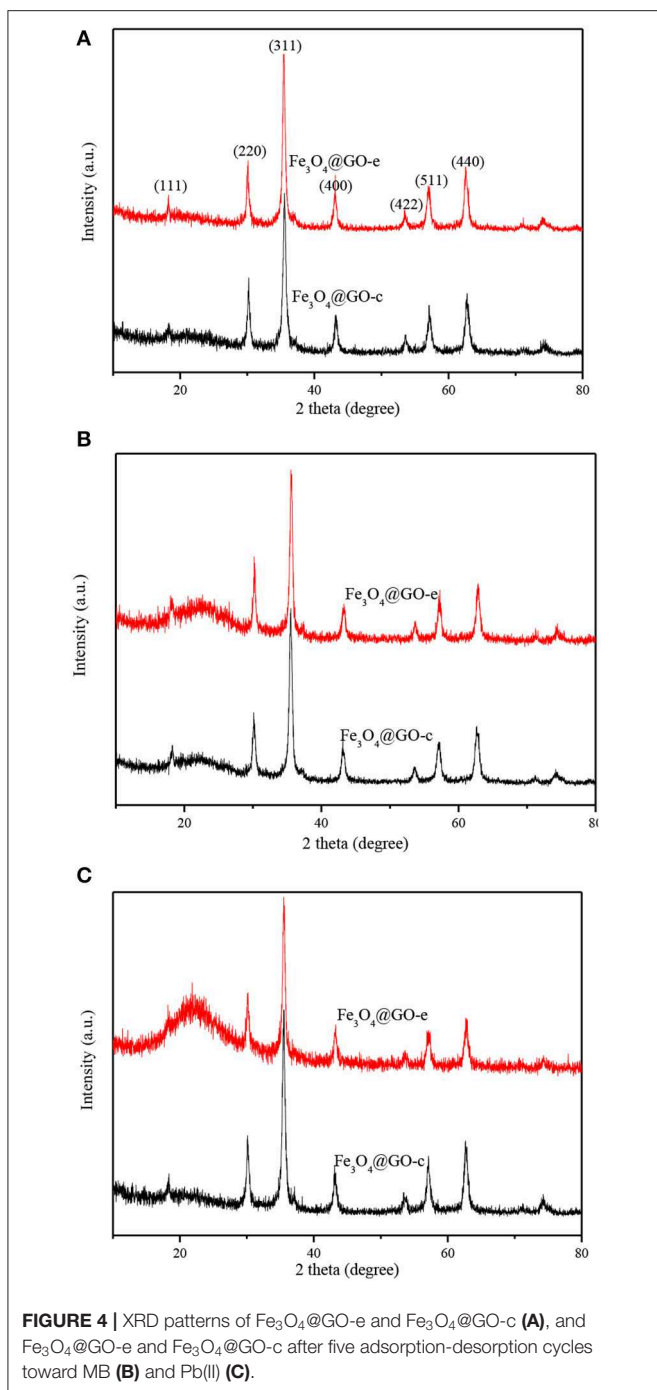
Nevertheless, the Fe₃O₄@GO-e sample had quite different morphologies and structures after adsorption-desorption recycling toward MB and Pb(II). From **Figure 3b**, it can be seen that the morphology and core-shell structure of Fe₃O₄@GO-e are approximately preserved, manifesting that the Fe₃O₄@GO-e sample could keep stable during regeneration toward MB. However, after adsorption-desorption toward Pb(II), its morphology and structure had completely changed. **Figure 3d** clearly shows that the magnetic NPs are not wrapped by GO sheets and instead they lie on GO sheets via weak connection. The TEM image (**Figure 3f**) further shows that the GO sheets

have been almost separated from the magnetic NPs. Obviously, the Fe₃O₄@GO-e sample had disintegrated and its core-shell structure had been destroyed.

XRD and Magnetic Property Analyses

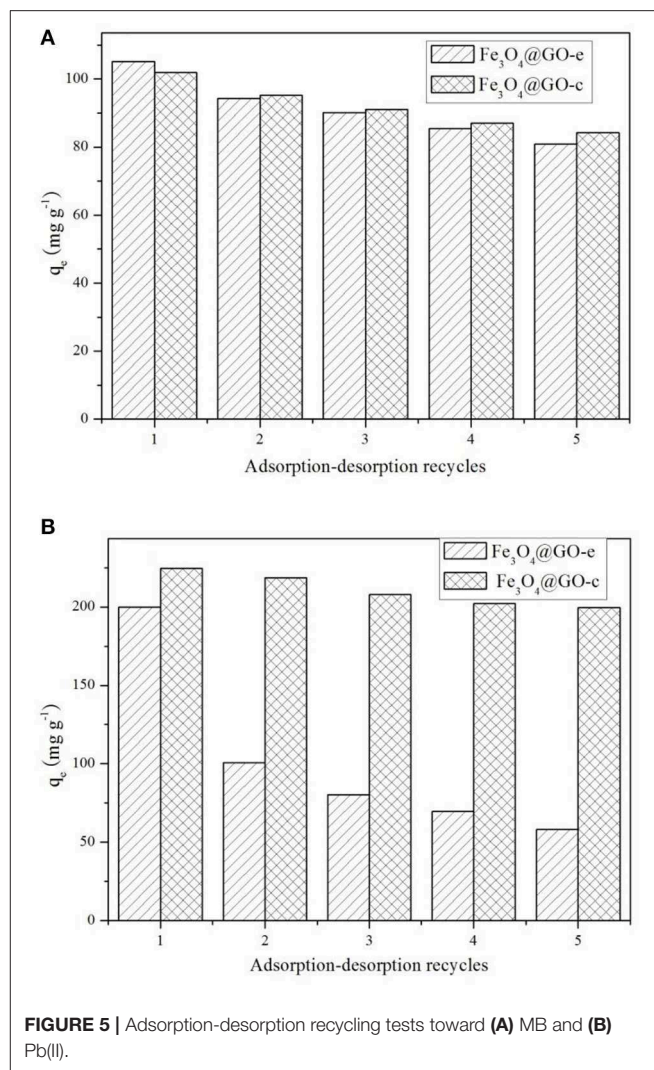
XRD technique is a powerful tool for structure characterization, and the structure variation of the Fe₃O₄@GO samples mainly lies in whether the GO sheets could still wrap the magnetic NPs or disintegrate from the NPs. The XRD patterns of Fe₃O₄@GO samples before and after recycling are shown in **Figure 4**. It is evident that all samples have the typical XRD pattern of magnetite (JCPDS No. 19-0629), indicating that the Fe₃O₄ NPs retain their original crystalline structure. It should be paid attention to the peaks variation at the 2θ range of 20–30° for the magnetic GO composites. The composites tend to appear with a broad XRD peak at 20–30° when metal NPs are deposited on the graphene sheets, which is due to the loose stacking of graphene sheets (Ai et al., 2011; Guo et al., 2015; Wu et al., 2016). However, in our case, there existed almost no peak at 20–30° for the Fe₃O₄@GO samples (**Figure 4A**). It could be explained that the peak at 20–30° is attributed to the stacking of the tiled GO sheets, which would disappear for the wrapped GO sheets. As for the regenerated samples, their XRD patterns are very different from the aboves. From **Figure 4B**, it could be seen that the regenerated Fe₃O₄@GO-c sample has a negligible peak whereas the regenerated Fe₃O₄@GO-e has a tiny peak at 20–30°. It could be deduced that the core-shell structure of Fe₃O₄@GO-c could be well maintained and Fe₃O₄@GO-e could generally preserve the core-shell structure during regeneration toward MB. However, after desorbing Pb(II), the Fe₃O₄@GO-e sample displays an intensive and broad peak at 20–30° (**Figure 4C**), manifesting that most GO sheets are separated from the magnetic NPs. On the contrary, the XRD peak of Fe₃O₄@GO-c are almost same as that in **Figure 4A**, verifying that it could well maintain core-shell structure during adsorption-desorption of Pb(II). The XRD results inherently reveal the structure evolution of Fe₃O₄@GO during adsorption-desorption process, which are highly consistent with the SEM/TEM characterizations. The results further clarify the structure evolution of the Fe₃O₄@GO samples during adsorption-desorption process.

The magnetism of novel carbon materials plays a pivotal role for their application as adsorbents (Ren et al., 2019; Zhang et al., 2019). The maximum saturation magnetizations of the GO-based samples are listed in **Table 1**, from which it could be seen that they change slightly after five cycles of adsorption-desorption toward MB or Pb(II). The negligible variation in magnetization can be deduced that the magnetism of the samples comes from Fe₃O₄ NPs and they are well-preserved in the samples after recycling. The good magnetization is very helpful to facilitate the post-processing of the GO composites. However, after desorption-desorption of Pb(II), the Fe₃O₄@GO-e sample has completely disintegrated its core-shell structure. As a result, a mixture of magnetic NPs and GO sheets was formed, therefore, it had to be separated from solution by membrane filtration instead of external magnet.



Regeneration Study

The adsorption-desorption tests for the samples were repeated five times using MB and Pb(II) as the adsorbates, and the results are displayed in **Figure 5**. Before recycling, Fe₃O₄@GO-e exhibits an adsorption capacity of 105.5 mg/g toward MB, which is a little higher than Fe₃O₄@GO-c (102.4 mg/g). However, Fe₃O₄@GO-c displays a greater initial adsorption amount (224.5 mg/g) than Fe₃O₄@GO-e (199.8 mg/g). It could be attributed to the fact that Fe₃O₄@GO-c is rich

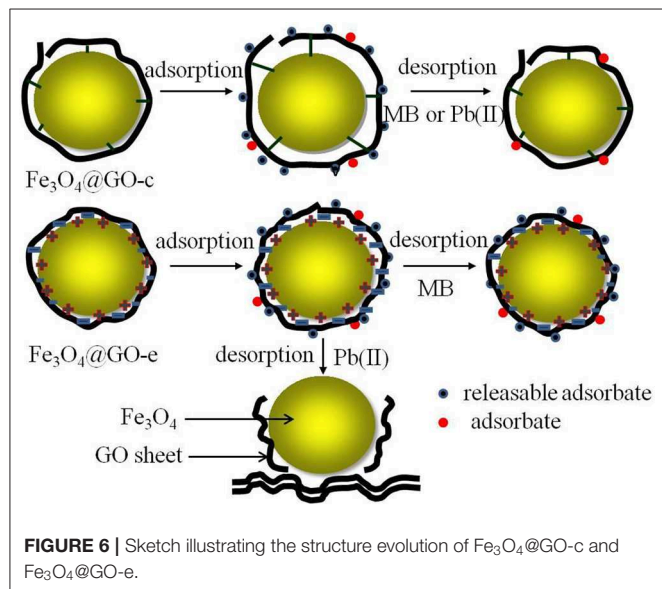


of -NH₂ groups, which can help to chelate Pb(II). From **Figure 5A**, it could be observed that both of the Fe₃O₄@GO samples could maintain good regeneration even after five cycles toward MB, and the Fe₃O₄@GO-e and Fe₃O₄@GO-c samples could hold 77% and 83% adsorption capacities, respectively. Nevertheless, the samples present very different regeneration performances toward Pb(II). From **Figure 5B**, it could be seen that Fe₃O₄@GO-c could maintain ~89% adsorption capacity after five cycles whereas Fe₃O₄@GO-e only possesses ~29% adsorption capacity. Moreover, for the initial cycle, the adsorption capacity of Fe₃O₄@GO-e has been drastically decreased, inferring that its structure has greatly changed.

It is well-known that the performance of a composite is highly related to its structure. Therefore, it could be reasonably deduce that the significant variation of the Fe₃O₄@GO-e sample in adsorption capacity toward Pb(II) is attributed to the disintegration of its core-shell structure. Indeed, during desorption of Fe₃O₄@GO-e toward Pb(II), there existed black

TABLE 1 | The maximum saturation magnetisms of the Fe₃O₄@GO samples before and after five cycles of adsorption-desorption toward MB and Pb(II).

Samples	No recycling	After five cycles toward MB	After five cycles toward Pb(II)
Fe ₃ O ₄ @GO-e	61.0	59.5	59.1
Fe ₃ O ₄ @GO-c	57.1	55.8	55.3

**FIGURE 6** | Sketch illustrating the structure evolution of Fe₃O₄@GO-c and Fe₃O₄@GO-e.

GO sheets in solution, which could not be separated by an external magnet, fully demonstrating that the GO sheets had been separated from the composites and dispersed in solution. The slight decrement in adsorption capacities in other cases could be explained that the pre-adsorbed amounts could not be totally released from adsorption sites (Zhang et al., 2013), hence verifying that their core-shell structures had been well-preserved. In this study, only Pb(II) was used for the investigation, but, as a typical heavy metal ion, the related results may be applied to other heavy metal ions because they had a similar adsorption mechanism by Fe₃O₄@GO-e and other GO-based adsorbents (Hu et al., 2017).

Structure Evolutions of the Fe₃O₄@GO Samples During Regeneration Process

The structure evolution of the adsorbents during regeneration is closely related to their regeneration performance. Therefore, it is very beneficial to improving the structural stability by adoption of pertinent measures.

In this study, both Fe₃O₄@GO samples have a similar core-shell structure, in which the magnetic NPs are tightly wrapped by GO sheets. However, the interactions between the core and shell are completely different, which are electrostatic and covalent. The Fe₃O₄@GO-c sample has a stable structure due to the firm covalent bonding that could resist the acid

and ethanol environment during regeneration, resulting in good regeneration performance toward MB and Pb(II). For the Fe₃O₄@GO-e sample, its structure is not very stable owing to the weak electrostatic connection, but it could still maintain its core-shell structure in ethanol solution, thus resulting in a reasonable regeneration performance toward MB.

Unfortunately, when desorbing Pb(II) in acid solution, the Fe₃O₄@GO-e sample would disassemble due to the following reasons: (1) H⁺ ions could attract GO sheets with negative charges; (2) A great number of H⁺ ions in solution could endow GO sheets with positive charges, and it would repel the magnetic NPs with the same charges. The sketch illustrating the structure evolution during regeneration is presented in Figure 6.

CONCLUSION

Two kinds of composites with the structure of GO sheets wrapped magnetic nanoparticles composites had been successfully synthesized, and their regeneration had been investigated using MB and Pb(II) as adsorbates. Both samples have a similar core-shell structure, and the linking forces between core and shell are electrostatic and covalent, respectively. During regeneration, the GO@Fe₃O₄-c sample could resist the erosion from ethanol and acid solution, and could well maintain its core-shell structure. After five cycles, it still holds the adsorption capacity ~83% toward MB and ~89% toward Pb(II), respectively. The GO@Fe₃O₄-e sample could preserve ~77% adsorption capacity toward MB, and could roughly keep the core-shell structure after five cycles. However, it would completely disassemble its core-shell structure, resulting in only ~29% adsorption capacity toward Pb(II) after five cycles. The related regeneration mechanism and the structure evolution during regeneration had been proposed, which could provide a theoretical guide for designing and improving the GO-based composites.

DATA AVAILABILITY STATEMENT

The datasets generated for this study are available on request to the corresponding author.

AUTHOR CONTRIBUTIONS

ZH and XZ conducted the most experiments. JL and YZ performed the characterization and data analysis. All authors involved the analysis of experimental data and manuscript preparation.

ACKNOWLEDGMENTS

The authors would like to acknowledge the financial support from the National Natural Science Foundation of China (Nos. 21576075, 21376069).

REFERENCES

- Ai, L., Zhang, C., and Chen, Z. (2011). Removal of methylene blue from aqueous solution by a solvothermal-synthesized graphene/magnetite composite. *J. Hazard. Mater.* 192, 1515–1524. doi: 10.1016/j.jhazmat.2011.06.068
- Bourlinos, A. B., Gournis, D., Petridis, D., Szabo, T., Szeri, A., and Dekany, I. (2003). Graphite oxide: chemical reduction to graphite and surface modification with primary aliphatic amines and amino acids. *Langmuir* 19, 6050–6055. doi: 10.1021/la026525h
- Chandra, V., Park, J., Chun, Y., Lee, J. W., Hwang, I. C., and Kim, S. (2010). Water-dispersible magnetite-reduced graphene oxide composites for arsenic removal. *ACS Nano* 4, 3979–3986. doi: 10.1021/nn1008897
- Gao, J., Ran, X., Shi, C., Cheng, H., Cheng, T., and Su, Y. (2013). One-step solvothermal synthesis of highly water-soluble, negatively charged superparamagnetic Fe₃O₄ colloidal nanocrystal clusters. *Nanoscale* 5, 7026–7033. doi: 10.1039/c3nr00931a
- Geim, A. K., and Novoselov, K. S. (2007). The rise of graphene. *Nat. Mater.* 6, 183–191. doi: 10.1038/nmat1849
- Guo, L., Ye, P., Wang, J., Fu, F., and Wu, Z. (2015). Three-dimensional Fe₃O₄-graphene macroscopic composites for arsenic and arsenate removal. *J. Hazard. Mater.* 298, 28–35. doi: 10.1016/j.jhazmat.2015.05.011
- He, F., Fan, J., Ma, D., Zhang, L., Leung, C., and Chan, H. (2010). The attachment of Fe₃O₄ nanoparticles to graphene oxide by covalent bonding. *Carbon* 48, 3039–3144. doi: 10.1016/j.carbon.2010.04.052
- Hu, Z., Aizawa, M., Wang, Z., and Hatori, H. (2009). Palladium precursor for highly-efficient preparation of carbon nanosheet-palladium nanoparticles composites. *Carbon* 47, 3365–3380. doi: 10.1016/j.carbon.2009.08.008
- Hu, Z., Aizawa, M., Wang, Z., Yoshizawa, N., and Hatori, H. (2010). Synthesis and characteristics of graphene oxide-derived carbon nanosheet-Pd nanosized particle composites. *Langmuir* 26, 6681–6688. doi: 10.1021/la9040166
- Hu, Z., Chen, Y., Hou, Q., Yin, R., Liu, F., and Chen, H. (2012). Characterization of graphite oxide after heat treatment. *New J. Chem.* 36, 1373–1377. doi: 10.1039/c2nj20833d
- Hu, Z., Qin, S., Huang, Z., Zhu, Y., Xi, L., and Li, Z. (2017). Recyclable graphene oxide-covalently encapsulated magnetic composite for highly efficient Pb(II) removal. *J. Environ. Chem. Eng.* 5, 4630–4638. doi: 10.1016/j.jece.2017.09.003
- Hu, Z., Zhang, X., Cui, H., and Li, Z. (2020). Novel magnetic nanocluster@graphene oxide composites for potential application in environmental adsorption. *J. Nanosci. Nanotechnol.* 20, 1814–1821. doi: 10.1166/jnn.2020.17357
- Hummers, W. S., and Offeman, R. E. (1958). Preparation of graphite oxide. *J. Am. Chem. Soc.* 80, 1339–1339. doi: 10.1021/ja01539a017
- Li, M., Liu, Y., Zeng, G., Liu, N., and Liu, S. (2019). Graphene and graphene-based nanocomposites used for antibiotics removal in water treatment: a review. *Chemosphere* 226, 360–380. doi: 10.1016/j.chemosphere.2019.03.117
- Liu, X., Xu, X., Sun, J., Alsaedi, A., Hayat, T., Li, J., et al. (2018). Insight into the impact of interaction between attapulgite and graphene oxide on the adsorption of U(VI). *Chem. Eng. J.* 343, 217–224. doi: 10.1016/j.cej.2018.02.113
- Ma, Y., Shao, W., Sun, W., Kou, Y., Li, X., and Yang, H. (2018). One-step fabrication of β -cyclodextrin modified magnetic graphene oxidenanohybrids for adsorption of Pb(II), Cu(II) and methylene blue in aqueous solutions. *Appl. Surf. Sci.* 459, 544–553. doi: 10.1016/j.apsusc.2018.08.025
- Mi, X., Huang, G., Xie, W., Wang, W., Liu, Y., and Gao, J. (2012). Preparation of graphene oxide aerogel and its adsorption for Cu²⁺ ions. *Carbon* 50, 4856–4864. doi: 10.1016/j.carbon.2012.06.013
- Nandhanapalli, K. R., Mudusu, D., and Lee, S. (2019). Functionalization of graphene layers and advancements in device applications. *Carbon* 152, 954–985. doi: 10.1016/j.carbon.2019.06.081
- Pan, S., Chen, X., Shen, H., Li, X., Cai, M., Zhao, Y., et al. (2016). Rapid and effective sample cleanup based on graphene oxide-encapsulated core-shell magnetic microspheres for determination of fifteen trace environmental phenols in seafood by liquid chromatography tandem mass spectrometry. *Anal. Chim. Acta* 919, 34–46. doi: 10.1016/j.aca.2016.02.035
- Ren, L., Lin, H., Meng, F., and Zhang, F. (2019). One-step solvothermal synthesis of Fe₃O₄@carbon composites and their application in removing of Cr(VI) and Congo red. *Ceram. Int.* 45, 9646–9652. doi: 10.1016/j.ceramint.2018.11.132
- Sitko, R., Turek, E., Zawisza, B., Malicka, E., Talik, E., Helmann, J., et al. (2013). Adsorption of divalent metal ions from aqueous solutions using graphene oxide. *Dalton Trans.* 42, 5682–5689. doi: 10.1039/c3dt33097d
- Smith, S. C., and Rodrigues, D. F. (2015). Carbon-based nanomaterials for removal of chemical and biological contaminants from water: a review of mechanisms and applications. *Carbon* 91, 122–143. doi: 10.1016/j.carbon.2015.04.043
- Wei, H., Yang, W., Xi, Q., and Chen, X. (2012). Preparation of Fe₃O₄@graphene oxide core-shell magnetic particles for use in protein adsorption. *Mater. Lett.* 82, 224–226. doi: 10.1016/j.matlet.2012.05.086
- Wu, X., Shi, Y., Zhong, S., Lin, H., and Chen, J. (2016). Facile synthesis of Fe₃O₄-graphene@mesoporous SiO₂ nanocomposites for efficient removal of methylene blue. *Appl. Surf. Sci.* 378, 80–86. doi: 10.1016/j.apsusc.2016.03.226
- Yoon, Y., Park, W. K., Hwang, T. M., Yoon, D. H., Yang, W. S., and Kang, J. W. (2016). Comparative evaluation of magnetite-graphene oxide and magnetite-reduced graphene oxide composite for As(III) and As(V) removal. *J. Hazard. Mater.* 304, 196–204. doi: 10.1016/j.jhazmat.2015.10.053
- Zhang, J., Zhai, S., Li, S., Xiao, Z., Song, Y., An, Q., et al. (2013). Pb(II) removal of Fe₃O₄@SiO₂-NH₂ core-shell nanomaterials prepared via a controllable sol-gel process. *Chem. Eng. J.* 215–216, 461–471. doi: 10.1016/j.cej.2012.11.043
- Zhang, M., Ma, X., Li, J., Huang, R., Guo, L., Zhang, X., et al. (2019). Enhanced removal of As(III) and As(V) from aqueous solution using ionic liquid-modified magnetic graphene oxide. *Chemosphere* 234, 196–203. doi: 10.1016/j.chemosphere.2019.06.057

Conflict of Interest: The authors declare that the research was conducted in the absence of any commercial or financial relationships that could be construed as a potential conflict of interest.

Copyright © 2020 Hu, Zhang, Li and Zhu. This is an open-access article distributed under the terms of the Creative Commons Attribution License (CC BY). The use, distribution or reproduction in other forums is permitted, provided the original author(s) and the copyright owner(s) are credited and that the original publication in this journal is cited, in accordance with accepted academic practice. No use, distribution or reproduction is permitted which does not comply with these terms.